DEVELOPMENT OF PROCESSING TECHNIQUES FOR ADVANCED THERMAL PROTECTION MATERIALS

(NASA-Ames Grant No. NAG2-848)

Annual Progress Report

June 1, 1996 - May 31, 1997

Report submitted to:

Dr. Daniel B. Leiser
Thermal Protection Materials and Systems Branch
NAS-Ames Research Center

Report submitted by:

Dr. Guna Selvaduray
Materials Engineering Department
San Jose State University

May 27, 1997

1996-1997 Annual Report

Guna Selvaduray, Jamie Lacson, and Julian Collazo
Department of Materials Engineering
San Jose State University
San Jose, CA 95192-0086

Introduction

During the period June 1, 1996 through May 31, 1997, the main effort has been in the development of materials for high temperature applications. Thermal Protection Systems (TPS) are constantly being tested and evaluated for thermal shock resistance, high temperature dimensional stability, and tolerance to environmental effects. Materials development was carried out by using many different instruments and methods, ranging from intensive elemental analysis to testing the physical attributes of a material.

The material development concentrated on two key areas: (1) development of coatings for carbon/carbon composites and (2) development of ultra-high temperature ceramics (UHTC). This report describes the progress made in these two areas of research during this contract period.

(1) Development of Protective Coatings for C/C Composites

The thermal and structural properties of C/C composites are ideal for many thermal protection applications. However, carbon is highly reactive in an oxidizing environment and must have a protective coating to insure its survival in a reentry environment. One potentially useful method of protecting these materials involves coating the surface with a polymer which is subsequently pyrolyzed to form an inert inorganic surface layer. Several polymers have been tested in an effort to produce an inert surface layer. It has been found that, under the pyrolysis conditions used so far, the surface layer contains a large amount of siliconoxycarbide (SiOC). It is important to

determine the composition of this pyrolysis product and then to correlate it with coating preparation procedures in order to develop more effective protective layers.

Several experimental methods have been used to examine the changes in composition of the polymer under different pyrolyzing conditions. These include Infrared (IR) spectroscopy, thermogravimetric analysis(TGA) and Inductively Coupled Plasma (ICP) emission spectroscopy. The ICP provides the best quantitative compositional data on these and other materials which contain boron, silicon, aluminum, and zirconium.

Colloidal Silica and Alumina Sol-Gel Experiments

Different mass concentrations of colloidal silica and alumina were mixed to develop top layer coatings for ceramic tiles. It is desired that 70 wt.% percent colloidal alumina and 30 wt.% colloidal silica (70/30 mixture) be mixed in a solution without gelling, so that it will not retain any water when the coating is applied to ceramic tiles. When a solution gels, it forms a hard cake with the total mass of the cake being much greater than the actual mass of silica and alumina contained in the solution. The extra weight is mostly water retained by the gel and is not desirable for ceramic coating. Coatings which retain water will add excess weight to the space shuttle.

AL20 (20 wt.% colloidal alumina in H_2O, pH =4.0) was mixed with NYACOL(34 wt.% colloidal silica in H_2O, pH=2.80) and Bindzil(40 wt.% silica and 4.0 wt.% alumina, pH = 3.56) in different ratios in an attempt to obtain a mixture that does not form a gel. Material balances were calculated for each mixture to obtain a 70/30 alumina/silica ratio.

After a series of experiments, it was found that gelling of the silica and alumina mixture was dependent upon pH and temperature. A viscometer was used to measure the increase in viscosity of the solution as it starts to gel with time. Solutions at room temperature gelled at a slower rate than solutions kept in an ice bath due to changes in pH from water evaporation. Colloidal silica had a greater impact on gelling than colloidal alumina did. In 50/50 mixtures, the time it took for a solution to gel was nearly three times faster than an 80/20 mixture. Solutions were also treated with aluminum hydroxide, sodium hydroxide, and potassium hydroxide to keep the pH of the mixture neutral.

Adding a base prevented the solution from gelling for a few days, after which the solutions started to thicken and gel.

Colloidal silica and alumina in powder form are currently being used to obtain the desired 70/30 mixture. Isobutyl alcohol is the solvent being used since it evaporates quickly. In a 200 ml glass beaker, about 7 grams of colloidal alumina and 3 grams of colloidal silica were mixed in 100 ml of isobutyl alcohol and mixed under turbulent regime and heated. After all the alcohol evaporated, the beaker contained only colloidal alumina and silica in powder form. The solution did not gel. There was no change in mass after the solvent had evaporated. A particle size analyzer was used to verify that the size of the particles did not change after being suspended in isobutyl alcohol. However, when the same mixture was kept at room temperature and was not continuously stirred, the solution gelled. Different solvents such as ethanol, isopropanol, and other high volatility solvents are being tested.

Surface Catalytic Efficiency of Advanced Carbon-Carbon TPS

Arcjet testing of several samples were recently completed in the Aero Heating Facility. The objective was to determine the catalytic efficiency(atom recombination coefficients for advanced carbon-carbon or ACC) on TPS. In order to accomplish this task, samples needed analyses before and after arcjet testing in order to investigate the material performance in aero heating environments.

The samples were disks, 0.060 cm thick and 7.11 cm in diameter, made from ACC and coated mainly with glass and/or silicon carbide. The carbon-carbon advanced technologies(C-CAT)-ACC-4 is an SiC conversion coating with a Type1 sealant, which is a sodium silicate based glass over a coating of tetraethylortho-silicate(TEOS). The Loral and Vought Process(LVP) is a silicon carbide over silicon boride glass containing zirconium oxide. This sample was provided by the Russians and was a CVD coating in a $SiC/HFBr_2$ system.

Platinum/Platinum-13%Rhodium thermocouples were installed either just behind the samples or in the surface area of the AETB insulation to hold them in place in the Arcjet testing. The samples were tested in the Arcjet and were analyzed using Scanning

Electron Microscopy(SEM), Energy Dispersive X-Ray analysis(EDX), and Inductively Coupled Plasma analysis(ICP).

Initial Arcjet exposures of the C-CAT and LVP samples resulted in a weight loss of 0.1% and 0.4% respectively. Upon further exposure of both samples in the Arcjet, a continuos weight gain occurred. Surface chemistry data showed the loss of sodium and carbon from the C-CAT sample, and of zirconium and oxygen form the LVP sample. The Russian sample remained relatively stable during Arcjet testing, as confirmed by SEM, DX, and ICP analyses.

Permeability Analysis For Tile Insulation[1]

Rigid fibrous refractory insulation (TPS tiles) are integral components of the thermal protection system of many hypersonic vehicles and spacecraft. These low density materials have open, highly porous microstructures consisting of interlaced ceramic fibers which typically take up less than 20% of the bulk insulation volume. The open porosity makes TPS tile materials permeable to gas flow. There are numerous instances in which internal gas transport in a thermal protection system could be important; examples include the penetration of hot boundary-layer gases, the flow of decomposition (pyrolysis) products, the use of convective flows to mitigate ice formation caused by cryopumping, and the design of refractory vents for pressure equilibration during atmospheric entry.

The permeability of the material to gas must be known to understand the gas flow through a porous solid; however, this property has not previously been available for the rigid fibrous insulation used in many thermal protection systems. Measurements of permeability for a variety of tile insulations, including materials from NASA's LI, FRCI, and AETB families are desired. This will enable correlationg the microstructure to the measured permeability.

The TPS materials tested include tiles from the LI, FRCI, and AETB families. LI-900 and LI-2200 tiles are composed of silica fibers, FRCI-12 tiles contain 80 w/o silica to

[1] Marschall, Jochen,, *Air Permeability of Rigid Fibrous Refractory Insulations*, 1996

20 w/o Nexel (aluminoborosilicate), FRCI-20 tiles contain 85 w/o silica to 15% Nextel, and the AETB-8, AETB-12, and AETB-20 tiles all consist of 68 w/o silica, 20 w/o alumina, and 12 w/o Nextel. Typical tile densities were less than 500 kg/m^3, and porosities generally exceed 80%.

Various combinations of pressure and flow rate, were achieved by adjustments of the leak valve and the throttling valve in the vacuum line were used. Measurements were made using the combination of pressure gauge and mass flow meter with the best operating range for the each experimental condition. Three type-K thermocouples were used, together with a Stanford Research Systems thermocouple monitor, to measure the ambient room temperature, the temperature of the inlet line, and the temperature of the brass test section. All the measurements obtained to date were made using ambient air as the test gas at temperatures in the range of 288 to 295 K.

The experimental set-up used to determine permeability is illustrated in Fig.1. Cylindrical specimens of various lengths where placed within a brass test section which was connected to a mechanical vacuum pump on one side and to a gas inlet line on the other. Three interchangeable test sections were available to accept samples with diameters of 2.54 cm, 1.796 cm, or 1.27 cm. The test sections were comprised of two parts, the longer of which could house specimens up to 8 cm in length. Samples were machined to fit tightly within the test section to mitigate gas leakage along the sides. Additionally, the interface between the sample and test section was overlapped on the downstream side by a silicon-rubber gasket which protruded about 0.02 cm into the bore of the test chamber. This gasket also served to seal the bolted flange connection between the two parts of the test section. Baratron-type capacitance manometer gauges (1000 torr, 100 torr, and 10 torr ranges) were used to measure the gas pressures upstream and downstream of the sample. A manifold with several on/off valves allowed the same pressure gauge to read both upstream and downstream pressures. Gases where introduced via a variable leak valve, and the flow rate was monitored using calibrated Tylan mass flow meters (30 sccm, 300 sccm, 1000 sccm, and 5000 sccm ranges). Various combinations of pressure and flow rate are achieved by adjustments of the leak valve and the throttling valve in the vacuum line. Measurements were made using the combination of pressure gauge and mass flow meter with the best operating range for the each

experimental condition. Three type-K thermocouples were used, together with a Stanford Research Systems thermocouple monitor, to measure the ambient room temperature, the temperature of the inlet line, and the temperature of the brass test section. All the measurements reported here were made using room air as the test gas at temperatures in the range of 288 to 295 K The experimental set-up used to determine permeability is illustrated in Figure1.

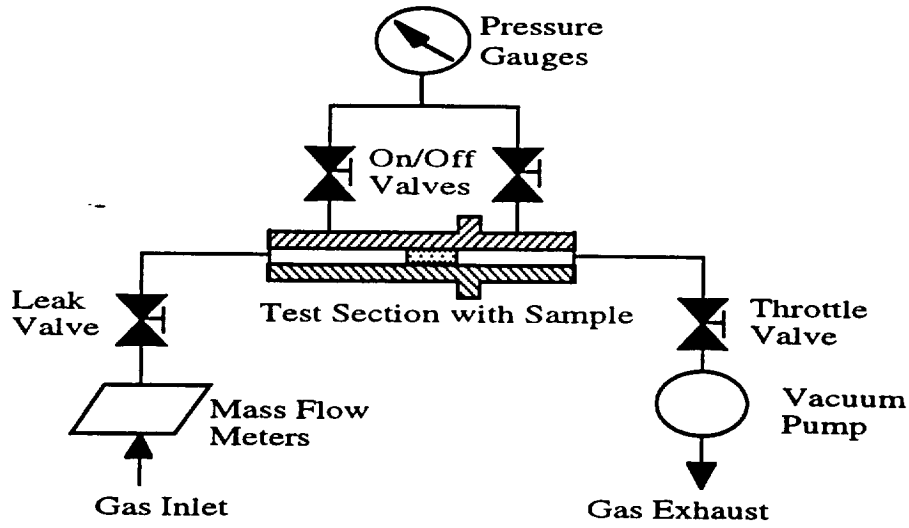

Figure 1. Experimental apparatus used to determine gas permeability of rigid fibrous insulations

In order to obtain the continuum flow permeability, K_o, and the permeability parameter, the experimental data are fitted using linear squares to the equation;

$$K_o[P_{ave} + b] = \frac{4\mu \dot{m} RTL}{\pi D^2 M \Delta P} \qquad \text{Eq.1}$$

where

b	permeability parameter
D	diameter, m
K_o	continuum flow permeability, m^2
L	length, m
M	molar mass, kg/kmol
$\dot{m}$	mass flow rate, kg/s
P_{ave}	$=(P_1 + P_2)/2$, Pa
R	universal gas constant, 8.314 J/mol-K
T	temperature, K
μ	viscosity, Pa-s

subscripts

1 downstream

2 upstream

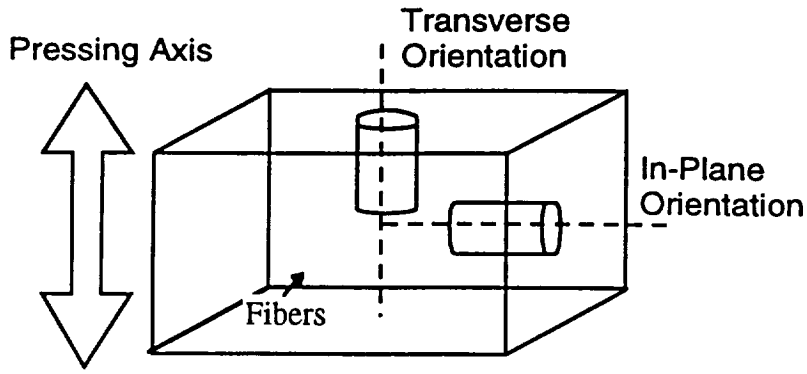

Figure 2. Orientation of the test specimens relative to the billet.

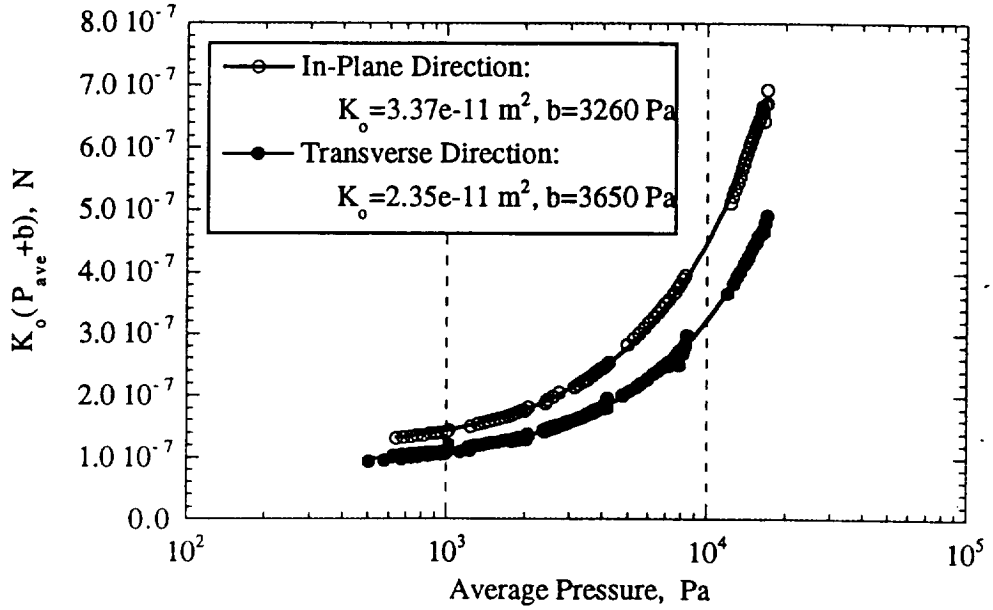

Figure 3. Comparison of experimental data for AETB-12 tile samples, tested along in-plane and transverse directions, with linear least-squares fits of Eq.(4). A log plot is used to separate data points.

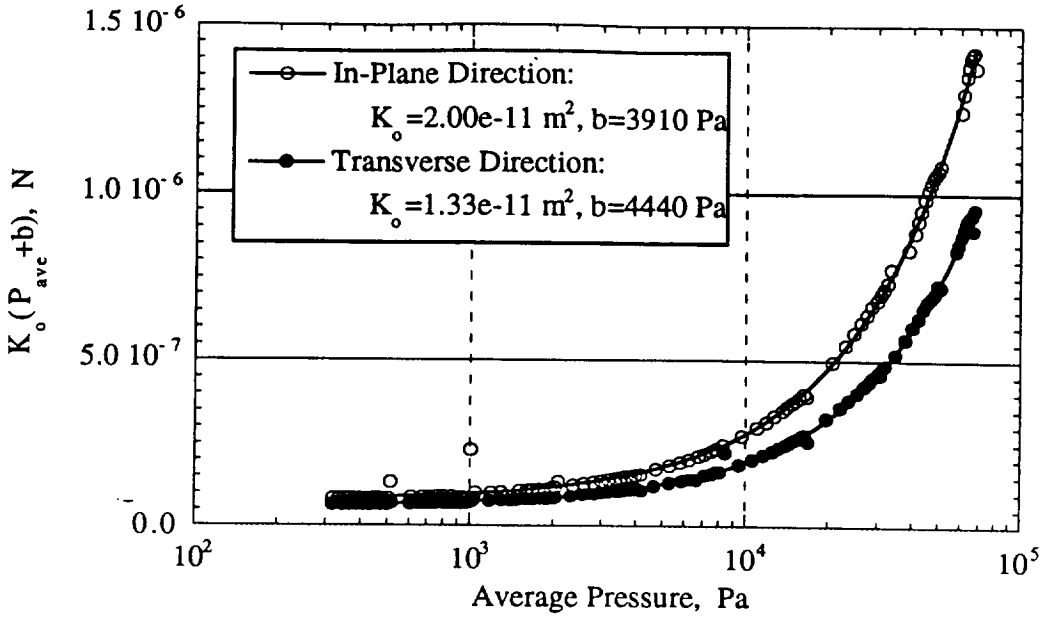

Figure 4. Comparison of experimental data for FRCI-12 tile samples, tested along in-plane and transverse directions, with linear least-squares fits of Eq.(4). A log plot is used to separate data points.

Figures 3 and 4 show experimental results for AETB-12 and FRCI-12, respectively. The data clearly show the influence of rarefied flow effects on permeability (non-zero y-intercept) and are fit very well by Equation 1. The data also reflect the microstructural anisotropy introduced during manufacture. The measured densities of the transverse and the in-plane oriented specimens compared in Figs. 3 and 3 differed by less 1%. Nevertheless, the ratio of the in-plane to the transverse values of K_o is about 1.4 for AETB-12 and 1.5 for FRCI-12. This difference is a direct consequence of the anisotropic fiber microstructure which projects a greater solid area on planes normal to the pressing axis than on planes parallel to it. Figure 2 shows the orientation of test samples in relation to the pressing axis. Flow in the transverse direction encounters more obstruction and must take a more tortuous path than flow in the in-plane directions to cover the same macroscopic distance.

The nominal density of an AETB-12 or an FRCI-12 tile is 12 lb/ft^3 (192.2 kg/m^3) however in practice the density of a particular specimen can vary by about ±1.5 lb/ft^3 (± 24.0 kg/m^3) owing to variations in bulk density among different billets because of subtle

processing deviations, as well as to density gradients within a given billet which are created in the pressing stage during manufacture. This behavior can be interpreted by considering the microstructural changes which occur as the density increases. A higher density means that more fibers are packed into the same macroscopic volume. The porosity and the characteristic pore size decrease. K_o falls because the total pore space available for flow is less and the flow path becomes more tortuous. Because the mean distance that a gas molecule can travel before striking a surface is also decreases, rarefied flow effects become important at higher pressures and consequently b increases.

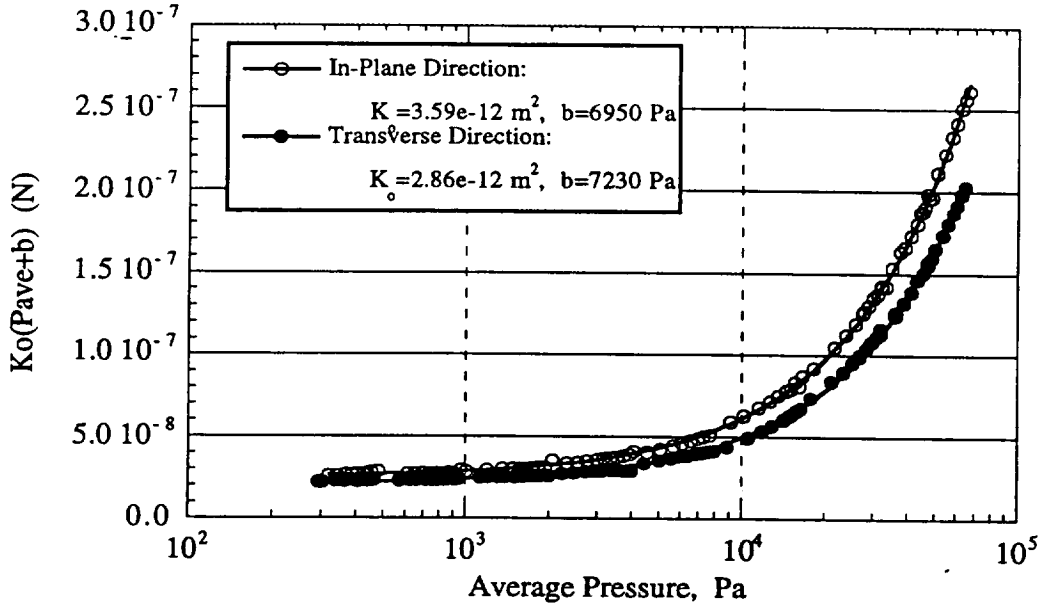

Figure 5. Comparison of experimental data for LI-2200 tile samples, tested along in-plane and transverse directions, with linear least-squares fits of Eq.(4). A log plot is used to separate data points.

Similarly for Figure 5, experimental results indicate that microstructural anisotropy from the manufacturing process affects the continuum flow permeability for the tile samples. For the in-plane direction, where fibers are perpendicular to the pressing axis, the flowing air undergo less obstruction. The in-plane orientation for LI-2200 is about 30% more permeable than samples tested with a transverse orientation.

Table 1. Experimental Results

	Transverse Orientation			In-Plane Orientation		
Material	r, kg/m^3	Ko, x10^{-12} m^2	b, Pa	r, kg/m^3	Ko, x10^{-12} m^2	b, Pa
LI-900	127	21.5	3910			
	130	19.6	4200			
	152	12.0	4940			
LI-2200	366	2.90	7640	380	3.59	6950
	370	2.86	7940	390	3.01	7430
	373	2.86	7230			
FRCI-12	197	14.8	4200	217	20.1	3740
	206	22.6	3620	217	20.0	3660
	213	14.3	4160			
	219	13.3	4440			
AETB-12	187	23.5	3650	187	33.7	3260
PICA	209	11.2	4630	217	40.5	1630
	211	11.6	4080	221	48.5	1620
	214	15.2	3420			

Table 1 is a comprehensive list of all the data gathered from the experimental apparatus in Figure 1. More samples from the AETB and PICA families are currently being tested. Different tile densities of LI-2200, LI-900, and FRCI-12 samples will also be tested through the end of 1997. Since rigid fibrous insulation are used in high temperature applications, an experimental apparatus is being developed that will allow for hot air(about 345-350K) to flow in the test section with the sample. The arc jet will be utilized in the development of an experiment to test porous ceramic heat vents for space probes. This will demonstrate that it is advantageous to use ceramic vents instead of refractory metals such as inconel because of its higher temperature melting point.

Oxidation Resistance Tests

The SEM has been utilized to support research of high temperature carbon materials. Carbon tiles and felts were coated with various materials to protect the carbon from oxidation under extreme conditions. The SEM with an energy dispersive x-ray analysis unit attached was employed to investigate the different phases present in the specimens. This led to the determination of whether or not the carbon was oxidized. To date, the carbon fibers have oxidized in all cases, and the research effort continues.

(2) Ultra High Temperature Ceramics (UHTC)

The materials development effort has focused on advanced UHTC materials that are borides and carbides of the group IV metals, and are capable of withstanding temperatures up to 3000°C in an aeroheating environment. These UHTC materials will allow development of new types of leading edge materials for hypersonic vehicles, allowing a sharper reentry trajectory.

Arc jet testing of several variations of materials was recently completed in the Aero Heating Facility (AHF) at Ames. The goal was to produce a material that had an oxidation layer that was thin, dense, and adherent. In order to accomplish this, samples needed analyses before and after arc jet testing in order to investigate material performance in aeroheating environments. The samples involved in this series of testing were 0.75 inch in diameter and 0.25 inch thick. Some of the specimens had a small hole bored, by Electric Discharge Machining (EDM), in the back-face, to a distance of within 1/32 of an inch from the front surface. A fiber optic sensor, mounted inside the model assembly, protruded into this hole and was used to measure the temperature. Other sensors were used to measure the temperature on the front surface of the specimen. The temperature differential across the thin oxide layer could then be determined by comparing the two measurements. The fiber optic sensor was also used to measure the back-face temperatures of specimens without in-depth holes. On the average, the oxide layers measured about 400 mm thick and had as much as a 300° C temperature drop across them. The measurements of the back-face temperature showed a 500-700° C temperature drop across the full 0.25" thick sample. Samples were analyzed using petrography, X-Ray Diffraction (XRD), SEM, Energy Dispersive X-Ray (EDX), IR, as well as other techniques. The ICP was also used to analyze unknown coatings formed on the arc jet model holders during testing. The analysis showed that the coatings were the result of out-gassing by one of the constituents of the sample. In addition, petrography techniques had to be developed to analyze the microstructure of the pre- and post-test arc jet samples. An optical microscope was used to analyze the steps in developing petrographic techniques. Upon completion of sample preparation, the microscope was used to obtain a photographic image for review and study. Analysis of the

microstructure showed that during processing, agglomerations formed between fine grained particles. These agglomerations caused highly porous regions that initiated failure and caused poor ablation performance. Therefore, work needs to be concentrated on improving the processing of these materials.

XRD analysis provided useful information in two areas. First, standard diffraction patterns were taken of each sample prior to testing to check for impurities and unexpected phase transformations that may have been produced in the processing stage. It was found that no new phases formed during processing and that impurities were negligible. Second, back-surface stress analysis of post-test samples was completed. To do this test, a different X-Ray tube had to be installed in the XRD. This required full readjustment and calibration of the machine. A powder sample containing the same material combination as the arc jet samples was analyzed to determine the baseline stress (A powder sample has a surface that is relatively stress free). After this analysis was completed, pre- and post-test samples were placed in the XRD unit to measure the back-surface stress due to arc jet testing. It was found that the back face of the post-test samples were in compression unexpectedly. XRD diffraction patterns were also taken on selected post-test samples to analyze the change in surface chemistry due to the formation of the oxidation layer. In the future, all test surfaces will be analyzed for determination of materials present before and after testing.

Flexural testing and analysis of UHTC materials, using four-point bending in accordance with MIL Standard 1942, were also completed. The relative strengths pertaining to different combinations of ZrB_2, ZrC, and SiC were evaluated. The relative strength of HfB_2/SiC was also examined. Pre-test analysis performed on each sample consisted of bulk density, and weight loss/gain measurements along with sonic modulus testing. The sonic modulus is used as a non-destructive technique to estimate Young's Modulus. It involves measuring the natural frequency of the material when it is tapped and converting that into a modulus taking into account the sample dimension and other material properties. Flexural testing was performed using a computer controlled Instron 1122 testing machine. Data received from the Instron's computer are in a form that is not easily transferable to other computer platforms, so macros were written in an EXCEL spreadsheet to analyze the data. These macros are adaptable to future testing programs.

Post-test analysis also involved doing petrography on specimens after fracture. From comparing micrographs to average strength, average density and SiC agglomeration formations, it was concluded that while additions of SiC helped to increase the average density and strength, porous agglomerations of SiC limited the strengths possible. It is known that a properly processed ZrB_2/SiC material can exhibit strengths on the order of 140 ksi. In this group of specimens the highest individual strength recorded was 108 ksi, but a high standard of deviation in strengths brought the average down to 45 ksi. This is attributed to a high quantity of SiC agglomerations that were formed during processing. However, these flexural bars were machined out of a scrap section of the pressing billet and are presumed to be a worst case scenario. The conclusion from flexural and Arc-Jet testing is that further work needs to be concentrated on the processing of these materials to improve the uniformity of the specimens and reduce SiC agglomerations.

A new all graphite model holder, coated with SiC for reusability, has also been designed for the next series of arc-jet testing. The purpose of the upcoming experiment is to measure the catalyticity of UHTC materials. The specimen size has been changed to 3" in diameter and 0.125" thickness. Holes, that come within 1/16 of an inch from the front-face of the sample, will be bored into the sample. More locations for fiber optic sensors have been added with the increase in diameter of the specimen. A total of five sensors can be implanted at one time as opposed to only one in previous testing. This additional capability will allow in-depth and back-face temperatures to be measured simultaneously. Testing is currently in progress and is expected to be completed during by the end 1997.